

Microstructure–fracture toughness correlation in weld joints of Cr–Mo steel

A. N. KUMAR, R. K. PANDEY, P. SUNDARAM

*Applied Mechanics Department, Indian Institute of Technology Delhi,
Hauz Khas, New Delhi 110016, India*

The strength–toughness–microstructure relationship in relation to the micromechanics of a fracture process has been investigated in the weld joints of two alloys: 0.5 Mo and 2.25 Cr–1 Mo steels. These alloys are extensively used to fabricate super-heater tubes, boilers, piping, gas lines, etc., by welding. The applications require high temperature and pressure to be maintained during service. The crack initiation toughness and tearing resistance were evaluated using crack tip opening displacement/ J -integral parameters at different temperatures. Quantitative analysis of micro-structure and fracture surfaces was used to study the micromechanics of fracture process in the heat-affected zone (HAZ) of the alloys. Molybdenum steel exhibited a higher percentage of ferrite and lower martensite content, while the other steel showed aligned carbide as the major constituent. The higher hardness and strength values in the HAZ and welding zone (WZ) of Cr–Mo steel, compared to molybdenum steel, may be attributed to the higher amount of martensite phase in the alloy. The higher initiation toughness at 200 °C in both the alloys was reflected in the larger dimple size, compared to the size observed at room temperature. A tendency for void sheet formation was noticed in both alloys. Acicular ferrite and martensite appeared to be the most influential constituents affecting tearing resistance and initiation toughness.

1. Introduction

Low alloy steels containing chromium and molybdenum are commonly used in situations where the components are exposed to high temperature and pressure during service. A few typical applications may include super-heater tubes in boilers, waste-heater boilers, tubes, piping and vessels for process gas lines, steam and process gas condensate, natural gas-lines, etc. Depending on the applications the pressure and temperature may vary over ranges of 40–300 kg mm⁻² and 10– + 550 °C, respectively. These structural alloys are often fabricated by a welding process which introduces varieties of micro-structural and compositional inhomogeneities, crack-like discontinuities and residual stresses [1–4]. The safety and integrity of welded structural components depends largely on the strength and toughness of various regions such as the weld zone (WZ), heat-affected zone (HAZ) and the parent metal (PM). In addition, the elevated temperature may also influence the behaviour of welded joints to a great extent.

The present investigation was conducted on two commonly used Cr–Mo alloys, i.e. 0.5 Mo steel and 2.25 Cr–1Mo steel to study the strength–toughness–microstructure relationship in the weldment of these alloys. The crack initiation toughness and the tearing resistance are characterized using crack tip opening displacement (CTOD) and J -integral parameters. The effect of temperature on crack-growth behaviour was also studied. The micromechanics of

crack initiation and growth has been investigated with the help of quantitative microstructural analysis and fractographic investigations. It was also the purpose of this investigation to identify the role of microstructure in influencing the stable tearing resistance and fracture toughness in the WZ and HAZ of the alloys.

2. Experimental procedure

The chemical analysis of the alloys investigated in the present work is reported in Table I. The plates of the alloys were welded by the manual metal arc welding (MMAW) process using low-hydrogen type electrodes.

The ASME Code was followed regarding welding technique, pre- and post-heat-treatment, selection of welding parameters, etc. Details of welding variables and conditions considered are reported elsewhere [1–3].

Single-edge notched (SEN) plate specimens of dimensions 12 mm × 24 mm × 125 mm and round tensile specimens of 5 mm diameter, were machined from the mid-section of the welded plate. The specimen length was made transverse to the welding direction. For testing of the weld section, it was ensured that the WZ lay at the middle of the specimen length. Details of specimen preparation for tensile and fracture toughness tests are given elsewhere [1–4]. The tensile and fracture mechanics tests were conducted at room temperature (30 °C) and at 200 °C. The ASTM

TABLE I Chemical composition (wt %)

Alloy	C	Mn	P	S	Si	Cr	Mo
SA 335 Gr. P1	0.21	0.81	0.034	0.023	0.255	0.22	0.45
SA 335 Gr. P22	0.14	0.48	0.035	0.026	0.330	2.07	0.86

TABLE II Tensile test results of as-received parent metal, WZ and HAZ

Alloy and condition	Test temperature (°C)	Yield strength (MPa)	Tensile strength (MPa)	Elongation (%)	Reduction in area (%)	Strain hardening exponent, <i>n</i>
Mo steel	PM 30	349	540	33	68	0.19
	WZ 30	520	613	25	69	0.08
	HAZ 30	360	560	26	72	0.18
	200	354	553	27	72	0.20
Cr-Mo steel	PM 30	389	566	33	78	0.17
	WZ 30	650	780	19	60	0.07
	HAZ 30	400	582	21	58	0.17
	200	352	551	20	58	0.19

standard [5] was followed for fracture mechanics tests where identically fatigue precracked SEN specimens were loaded to various load and displacement levels in an Instron machine. *In situ* heating was used for 200 °C temperature testing. Details of the testing procedure and heating arrangement are given elsewhere [1–4].

The experimental programme also included microstructural examination using an optical microscope, fracture surface examination using SEM, and hardness distribution across the WZ and HAZ using a Vickers hardness tester [3].

3. Results

3.1. Tensile properties and hardness distribution

The conventional tensile properties for the alloys are reported in Table II for the weld zone (WZ) and the heat-affected zone (HAZ), in addition to the parent metal (PM). The weld zone was found to exhibit higher strength than the as-received parent metal and the HAZ, for both alloys. Also, the HAZ appears to possess marginally higher strength and lower ductility than the PM in the alloys investigated.

The hardness distribution across the WZ and HAZ in both the steels is shown in Fig. 1. The maximum hardness was observed in the HAZ lying in the close vicinity of the WZ. The hardness values in Cr–Mo and 0.5 Mo steel were found to be around 300 and 270 VHN, respectively, as shown in Fig. 1. The strain hardening coefficient values are seen to be almost the same in PM and HAZ, while they are found to be quite low in the WZ for both alloys.

3.2. Critical *J* and CTOD values

The fracture toughness of the alloys was evaluated by measuring the critical values of CTOD and *J*-integral following BS5762 and ASTM E 813 [6, 7], respectively.

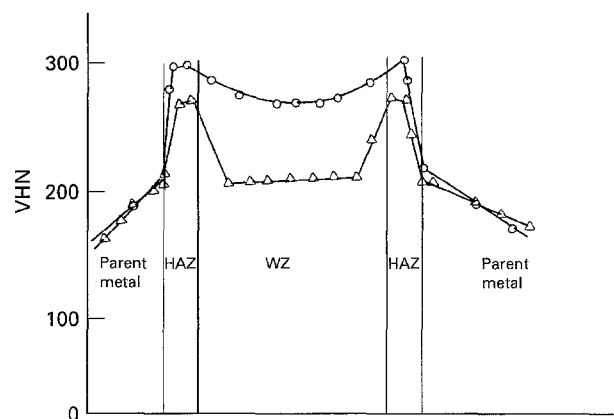


Figure 1 Hardness distribution across the welded plate for (○) Cr–Mo steel, and (△) molybdenum steel.

A crack growth resistance (*R*-curve) approach using the midthickness crack growth has been adopted here to find the critical values of CTOD and *J*-integral. A few typical *R*-curves are shown in Figs 2 and 3. The *R*-curves are found to be linear in almost all cases. The fracture toughness values were obtained from *R*-curves using two methods: (i) the blunting line equation where $\delta = 2\Delta a$ and $J = 2\sigma_0 a$ (values reported as the superscript *B*), and (ii) at a stretch zone width on *J*/ δ -*R* curves (values reported with superscript *S*). The fracture toughness values obtained for both the alloys are reported in Table III. The table also includes the experimentally measured stretch zone width and the δ_0 values at *a priori* crack growth, for comparison. The HAZ fracture toughness values were evaluated for both alloys at two temperatures, 30 and 200 °C. The WZ fracture toughness values were evaluated at only 30 °C for Cr–Mo steel. For comparison, the toughness values for molybdenum steel and Cr–Mo steel in the as-received condition, are also reported in Table III.

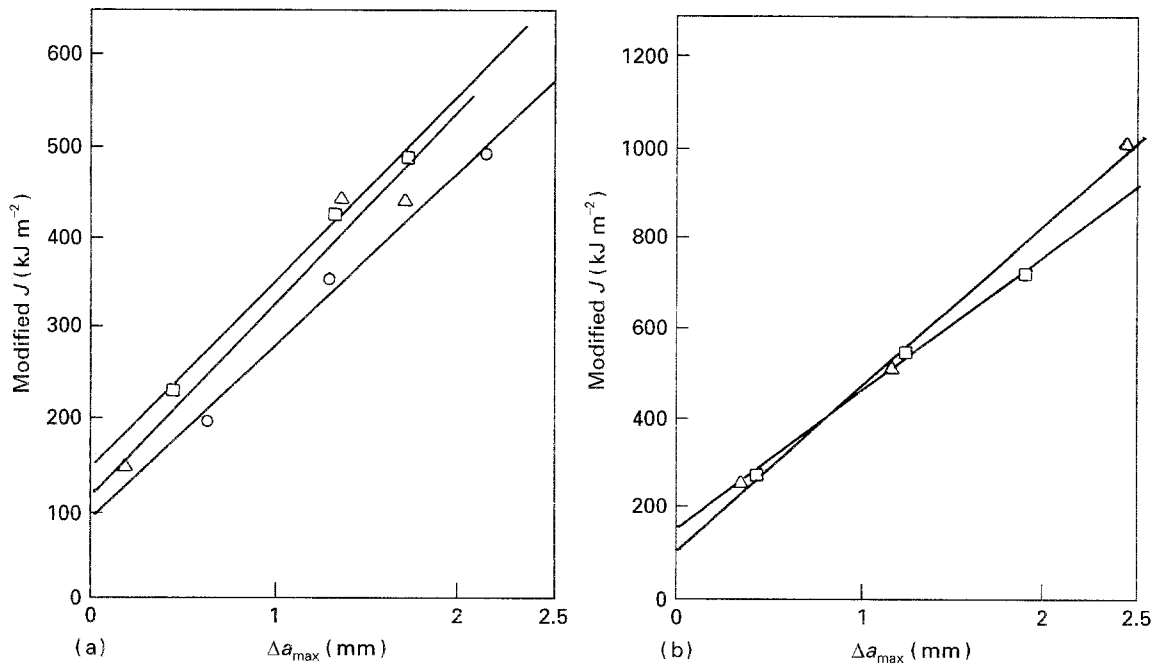


Figure 2 J - R curves for the weldments. (a) Cr-Mo steel: (O) WZ, 30°C; (Δ) HAZ, 30°C; (□) HAZ, 200°C. (b) Molybdenum steel: (Δ) HAZ, 30°C; (□) HAZ, 200°C.

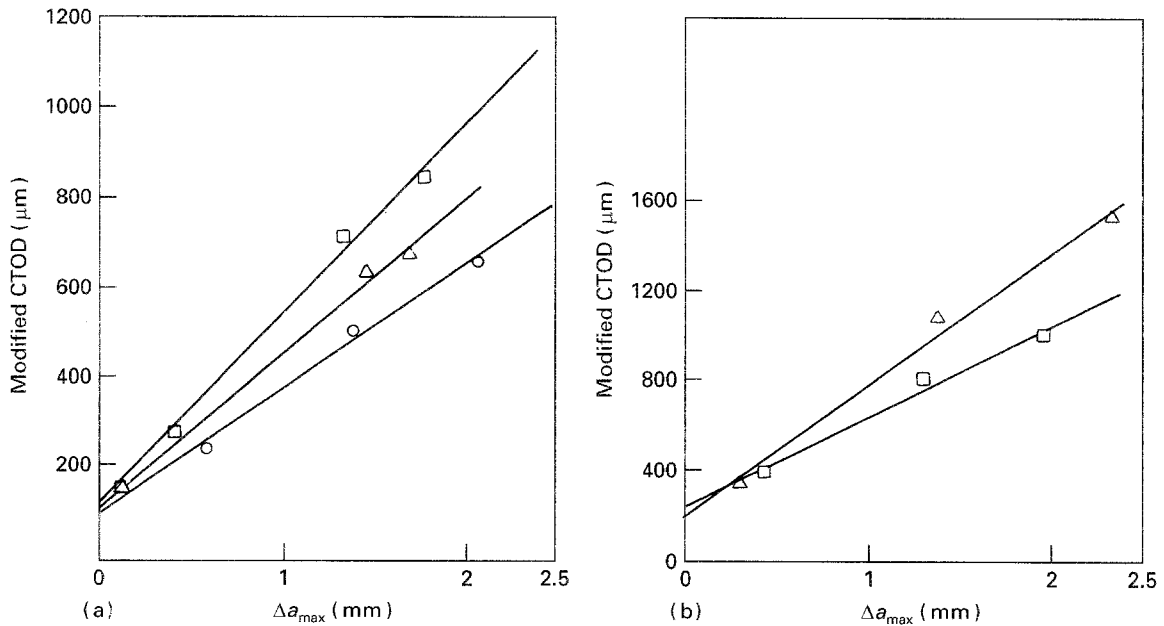


Figure 3 δ - R curves for the weldments. (a) Cr-Mo steel: (Δ) HAZ, 30°C; (□) HAZ, 200°C; (O) WZ, 30°C. (b) Molybdenum steel: (Δ) HAZ, 30°C; (□) HAZ, 200°C.

TABLE III Comparison of fracture initiation toughness values in the alloys

Alloy	Condition	Test temperature (°C)	J_{Ic}^B (kg mm ⁻²)	J_{Ic}^S (kg mm ⁻²)	δ_{Ic}^o (μm)	δ_{Ic}^B (μm)	δ_{Ic}^S (μm)	SZW (μm)
Mo steel	HAZ	30	183	161	205	295	280	129
	HAZ	200	241	210	234	295	295	151
Cr-Mo steel	WZ	30	110	107	97	115	119	80
	HAZ	30	142	135	109	135	140	91
	HAZ	200	192	175	126	157	178	125

3.3. Quantitative metallography

Quantitative information on the microstructure in three regions (WZ, HAZ and PM) was obtained through optical as well as scanning electron micro-

scopy [3, 4]. Some typical micrographs for various regions in the two alloys are shown in Fig. 4. The microstructural constituents observed are, polygonal ferrite (PF), acicular ferrite (AF), ferrite with aligned

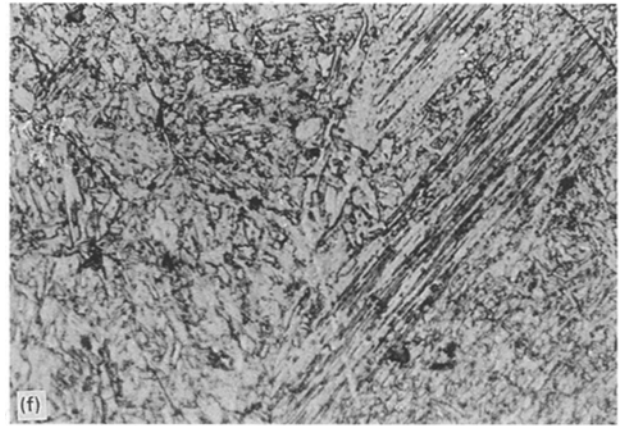
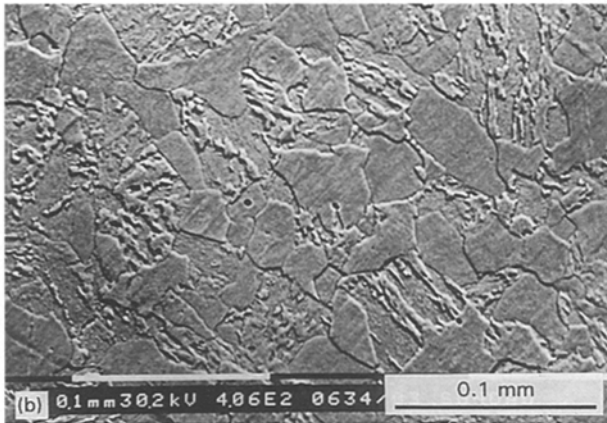
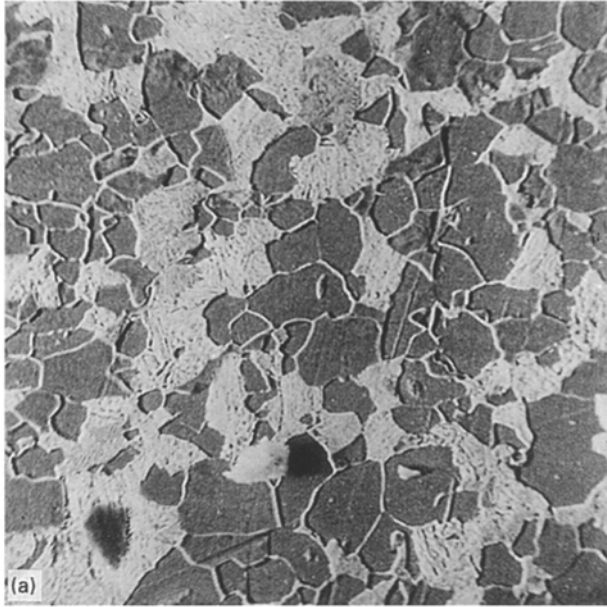


Figure 4 Typical micrographs of: (a) Molybdenum steel, as-received, $\times 560$; (b) Cr-Mo steel, as-received, $\times 406$; (c) Cr-Mo steel, WZ-HAZ, $\times 480$; (d) molybdenum steel, WZ, $\times 480$; (e) molybdenum steel, HAZ, $\times 350$; (f) Cr-Mo steel, WZ, $\times 480$.

martensite-austenite-carbide (AC), ferrite-cementite aggregate (FC) and martensite (M). The identification of the above constituents was based on the terminology as suggested earlier [8]. Table IV reports the results of quantitative analysis of microstructures in both alloys. An overall average value of the constituents is reported in the table.

4. Discussion

4.1. Weld zone and heat-affected zone microstructure

The WZ and HAZ in both alloys exhibit a composite and inhomogeneous microstructure that is different in many respects from the parent metal structures, as may be seen from Fig. 4. However, the reheating effect due to welding appears to be more distinct in molybdenum steel. While a uniform structure of HAZ over the thickness was noticed in Cr-Mo steel, at least four distinct regions, as schematically represented in Fig. 5, could be identified in the HAZ region of molybdenum steel. Region I, adjacent to WZ, corresponds to a less-hardening effect, while region II represents the reheated HAZ. Region III consists of the martensitic areas with minimum reheating effect, and region IV refers to the refined grain area of HAZ. The quantitative microstructural analysis was carried out over the four regions of HAZ and an overall proportion of the constituents was obtained by the weighted average of

TABLE IV Results of microstructural analysis

Alloy	Condition	Microstructural constituents (%)				
		PF	AF	AC	M	FC
Mo steel	WZ	23.6	67.4	6.6	–	2.4
	HAZ	3.8	43.0	22.0	30.0	1.2
Cr–Mo steel	WZ	5.8	57.2	36.0	–	1.0
	HAZ	7.5	19.5	24.5	47.0	1.5

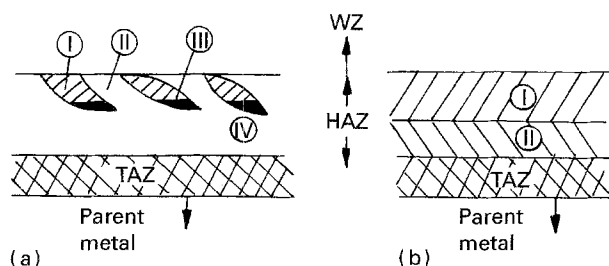


Figure 5 Schematic diagram showing variation of microstructures in the HAZ for (a) molybdenum steel, and (b) Cr–Mo steel.

areal fractions (Table IV). All four regions in molybdenum steel were found to be almost equally distributed over the HAZ. However, two main regions were displayed in Cr–Mo steel (Fig. 4), namely coarse martensite adjacent to the weld boundary, and a refined grain structure [3].

Table IV also reports the proportional distribution of various microstructural constituents in the WZ for both steels. A comparison of various constituents reveals that the HAZ of molybdenum steel contains relatively more AF ($\sim 43\%$) and less martensite ($\sim 30\%$) than the HAZ in Cr–Mo steel, although their total amount appears to be nearly the same (Table IV). The width of the lath martensite colony was found to be higher ($\sim 36\ \mu\text{m}$) in Cr–Mo steel than that of molybdenum ($\sim 25\ \mu\text{m}$). The polygonal ferrite in HAZ is in rather small proportion in both alloys [3]. On the other hand, the WZ microstructure displays somewhat higher acicular ferrite in both the steels, but the aligned carbide (AC) content is found to differ greatly, i.e. 36% and 6.6% in Cr–Mo and molybdenum steel, respectively. The higher manganese content in molybdenum steel ($\sim 0.81\%$) than Cr–Mo steel ($\sim 0.48\%$) might also have influenced the nucleation of ferrite grains and thus promoted higher AF content, suppressing coarse PF and GF [9].

4.2. Hardness–strength–microstructure relationship

The hardness in the HAZ of Cr–Mo steel is higher than the same in molybdenum steel and may be attributed to the presence of a greater proportion of lath martensite in the HAZ of Cr–Mo steel. The WZ hardness in both the alloys is attributed to the presence of AC, which is found to be substantially higher ($\sim 36\%$) in Cr–Mo steel, compared to the molybdenum steel ($\sim 6\%$).

The WZ exhibited higher strength than HAZ in both alloys. Also, the WZ of Cr–Mo steel showed a higher strength compared to molybdenum steel (Table II). However, the results should be visualized in the light of test limitations with the HAZ. As the HAZ is confined only over a narrow width around 2–3 mm along the WZ boundary of the test specimen, the tensile deformation and rupture would be influenced by the neighbouring zones, i.e. WZ and PM, and do not necessarily take place wholly within the HAZ.

4.3. WZ and HAZ fracture toughness

It may be seen from Table IV that J_{Ic} and δ_{Ic} values at *a priori* crack growth are significantly lower than the values obtained by other approaches. In general, for all the conditions studied, the difference in the critical J and δ values obtained by the blunting line method and the stretch zone width (SZW) method, is rather small. These two values (J_{Ic}^B/δ_{Ic}^B and J_{Ic}^S/δ_{Ic}^S) are considered to be appropriate crack initiation toughness for further discussions, because the other values appear to be unduly conservative and thus unrealistic. The HAZ toughness values reveal that an increase in temperature from 30 °C to 200 °C for both the alloys studied increases the fracture toughness significantly, irrespective of the measurement criterion used. The size of the SZW, as reported in the table, also increased by 20%–30% due to increased temperature. However, a different trend could be noticed in the crack growth resistance as characterized by tearing modulus, T_J and T_δ , and reported in Table V. The HAZ of molybdenum steel shows that at 200 °C the tearing modulus values are lower than those obtained at 30 °C. A comparison of two alloys indicated that the crack initiation toughness, as well as the tearing modulus values for the HAZ of Cr–Mo steel, are found to be lower compared to that of HAZ in 0.5 Mo steel at a given temperature. Also, the WZ toughness of Cr–Mo steel was found to be significantly smaller than the HAZ toughness.

4.4. Microstructural influence on toughness

An attempt has been made to interrelate fracture toughness with the corresponding microstructures of the alloys. From Tables III and IV it may be inferred that a higher proportion of AF and a relatively lower level of M in the HAZ of molybdenum steel, compared to the Cr–Mo steel, contribute to the higher initiation as well as crack growth toughness in this alloy. The

TABLE V Comparison of tearing modulus values in the alloys

Alloy	Condition	Test temperature (°C)	dJ/da (kg mm ⁻³)	T_J (°C)	$d\delta/da$	T_δ (°C)
Mo steel	HAZ	30	384	304	0.576	235
	HAZ	200	317	251	0.407	166
Cr–Mo steel	WZ	30	200	76	0.28	78
	HAZ	30	223	158	0.34	131
	HAZ	200	215	174	0.42	171

significant effect of AF on improving the fracture toughness was reported earlier [9–12]. The higher stretch zone width, which is related to the blunting of the crack tip and local plastic deformation as obtained in molybdenum steel, is also apparently due to the higher amount of AF present in the alloy.

In addition to the amount of M present, the width of an individual M colony may play a significant role in the crack tip deformation process, leading to crack initiation. The colony width of M in molybdenum steel is finer ($\sim 25 \mu\text{m}$) compared to that in Cr–Mo steel ($\sim 36 \mu\text{m}$). The lath martensite, because of its higher dislocation density and absence of twinning, is believed to be beneficial for enhanced crack initiation toughness [13]. However, the finer laths in molybdenum steel appears to make a greater contribution to toughness than the larger ones. In addition, the proportion of M laths contributes to the higher strength and hardness in Cr–Mo steel, thus impairing the fracture toughness. Similarly, fine acicular ferrite (2–6 μm in size) with random orientation in molybdenum steel, also offers higher resistance to tearing. An increased resistance to the cleavage mode of fracture and reduced ductile–brittle transition temperature by the AF structure, has been reported [14].

In the WZ in Cr–Mo steel, although the amount of AF present is considerably larger, a smaller toughness level is noticed. The major controlling factors in this case are presumably the pores, slag inclusions, coarse grains, etc., in the weld zone.

4.5. Micromechanics of crack initiation and propagation

An attempt was also made to study the micromechanics of cracking in the parent metal and HAZ through microfractographic investigations. In molybdenum steel and Cr–Mo steel, a microvoid coalescence mode resulting in dimpled fracture was observed. A few typical fractographs are shown in Fig. 6. An increase in the average size of dimples near the stretched zone (24 and 30 μm at 30 and 200 °C, respectively) in Cr–Mo steel is reflected in the increasing crack initiation toughness with temperature (Table IV). A similar dependency was also noticed in molybdenum steel where the average dimple size was found to increase from 28 μm to 42 μm when the temperature was increased from 30 °C to 200 °C. A decrease in initiation toughness was reported earlier with increase in test temperature in molybdenum steel. Metallographic studies around the stretch zone revealed

a progressively greater amount of grain deformation with increasing temperature in Cr–Mo steel, which resulted in increased strain hardening and energy dissipation. However, the molybdenum steel exhibited a reverse trend. For both the steels, the macroscopic fracture behaviour at various temperatures is reflected in the microscopic and fractographic observations.

A tendency for void-sheet formation around the slow crack growth region was observed in both steels. Fig. 6 shows void sheet formation through small second-phase particles spanning larger voids, which were possibly initiated at large inclusions. Because the molybdenum steel revealed a greater tendency for void sheet formation than the Cr–Mo steel, the former exhibited somewhat higher crack growth resistance [3]. The increasing test temperature facilitated the formation of void sheet around a slow crack growth region, resulting in decreasing tearing modulus in Cr–Mo steel [3]. The ease of void sheet formation in molybdenum steel may be attributed to the greater proportion of carbides because of the higher carbon content, compared to the carbides present in Cr–Mo steel. In addition, the higher value of strain hardening exponent in the molybdenum steel increased the crack tip triaxiality which appeared to enhance the nucleation, growth and coalescence of voids.

The fractographic investigation was also conducted in the HAZ fracture region which is represented in Fig. 6. Both the stretched zone (crack initiation region) and slow crack growth regions exhibited larger and deeper dimples in molybdenum steel than the dimple size observed in Cr–Mo steel. The void sheet formation was also noticed in HAZ fracture. The crack initiation, as well as crack-growth toughness in HAZ in both the steels, were found to be consistent with the dimple size, as observed earlier in the as-received condition [1–4].

5. Conclusions

The following conclusions may be drawn from the present investigation on 0.5 Mo steel and Cr–Mo steel.

1. The quantitative microstructural analysis of HAZ reveals a higher percentage of acicular ferrite and lower martensite content in molybdenum steel, compared to the Cr–Mo steel. The weld zone in Cr–Mo steel, on the other hand, exhibits a higher proportion of aligned carbide (AC) and a smaller proportion of PF than that of Mo steel.

2. Higher hardness and strength are noticed in the HAZ and WZ of Cr–Mo steel compared to the

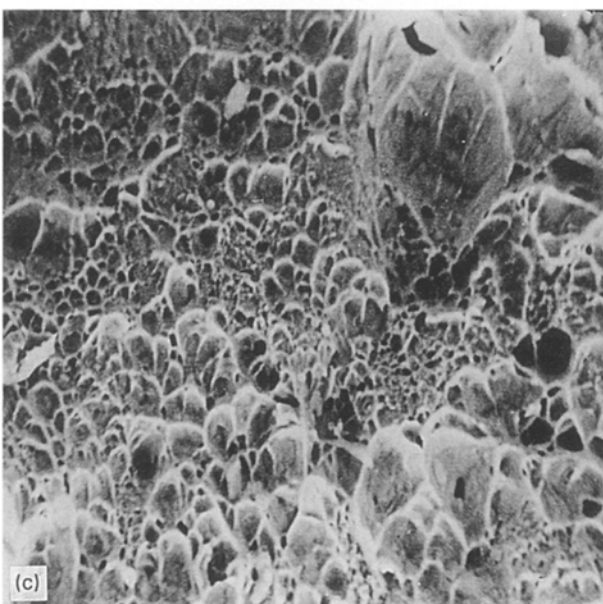
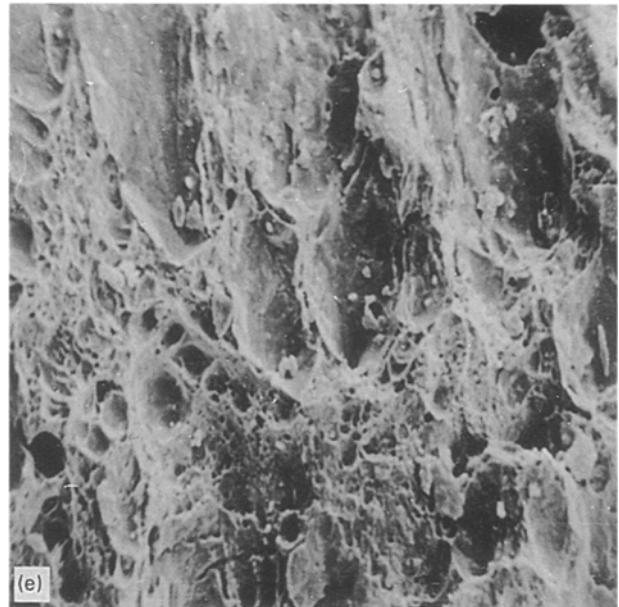
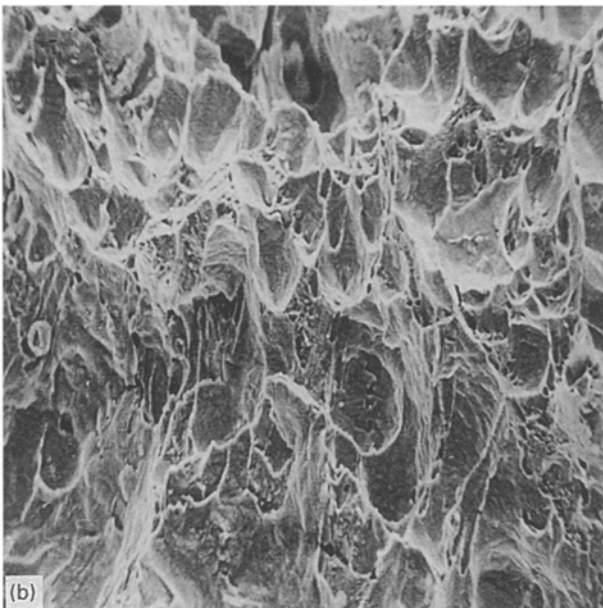
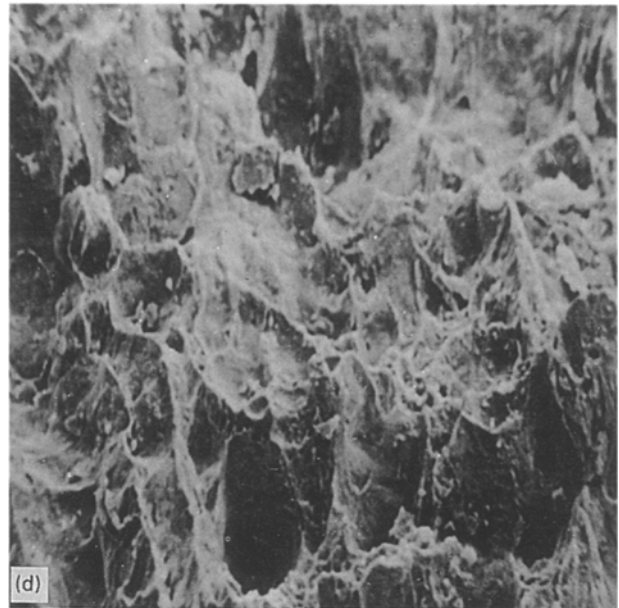
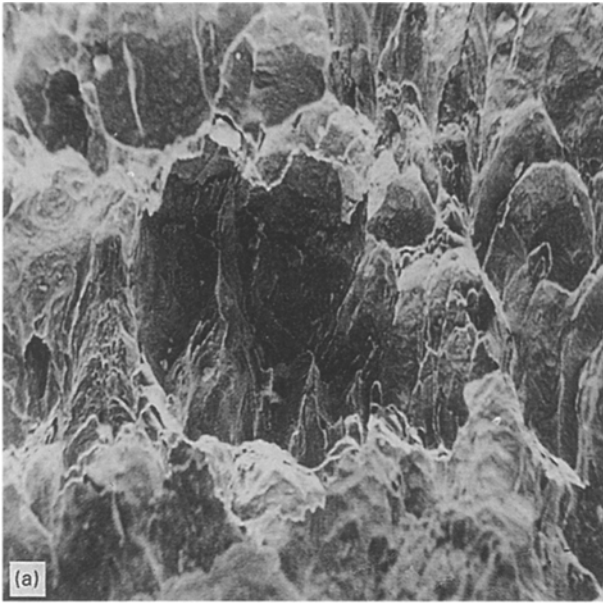


Figure 6 Typical microfractographs of: (a) AR Cr-Mo steel at 30°C, $\times 200$; (b) AR molybdenum steel at 30°C, $\times 400$; (c) AR molybdenum steel at 200°C, $\times 825$; (d) HAZ Cr-Mo steel at 30°C, $\times 41.5$; (e) HAZ molybdenum steel at 30°C, $\times 480$.

molybdenum steel. This may be attributed to the higher amount of martensite in the HAZ of Cr-Mo steel. The strength level, on the other hand, was found to be higher in the WZ than the respective HAZ in both alloys, because of the greater proportion of AF in molybdenum steel and more AF and AC in Cr-Mo steel.

3. AF and M appear to be the two most influential microstructural constituents affecting both the crack initiation toughness and the tearing modulus in the alloys studied. Higher AF and lower M content in the HAZ of molybdenum steel, compared to Cr-Mo steel accounts for the higher toughness in the alloys.

4. The increase in dimple size in the crack initiation zone accounts for increasing fracture toughness with temperature in both alloys. A tendency for void sheet

formation was observed in both the alloys. The ease of void sheet formation in molybdenum steel may be attributed to the greater proportion of carbides in the alloy.

References

1. R. E. RAI, P. SUNDARAM, R. K. PANDEY, A. N. KUMAR, S. K. BANERJEE and S. K. GHOSH, *Eng. Fract. Mech.* **37** (1990) 163.
2. V. R. RANGANATH, A. N. KUMAR and R. K. PANDEY, *Mater. Sci. Eng.* **A132** (1991) 152.
3. P. SUNDARAM, PhD thesis, Indian Institute of Technology, Delhi (1989).
4. P. SUNDARAM, R. K. PANDEY and A. N. KUMAR, *Mater. Sci. Eng.* **91** (1987) 29.
5. "Annual Book of ASTM Standards", Part 31 (American Society for Testing and Materials, Philadelphia, PA, 1973) p. 960.
6. British Standards Institution Document, BS5762, "Methods for COD Testing" (BSI, 1979).
7. "Standard Test for J_{IC} : A Measure of Fracture Toughness", ASME E-813-81 (ASME, 1981).
8. D. J. ABSON and R. E. DOLBY, "A Schematic for the Quantitative Description of Ferritic weld Metal", Report DCC IXJ-29-80 (Welding Institute, UK, 1980).
9. S. HOEKSTRA, *Met. Construct.* **18** (1986) 771.
10. S. K. CHAUDHARI and V. RAMASWAMY, in "Proceedings of ICF5", France (Pergamon Press, 1981) p. 1209.
11. C. L. CHOI and D. L. HILL, *Weld. J.* **57** (1978) 232.
12. H. G. PISARSKI and R. J. PARGETER, in "Proceedings of the International Conference on Welding in Energy Related Projects" (1983) pp. 415-28.
13. C. THAULOW, *Met. Const.* **17** (1985) 94.
14. K. ERIKSSON, in "Proceedings of ICFS", France (Pergamon Press, 1981) p. 715.

*Received 16 November 1993
and accepted 9 January 1995*